

# Spectral dependence of temporal point spread functions in human tissues

M. Essenpreis, C. E. Elwell, M. Cope, P. van der Zee, S. R. Arridge, and D. T. Delpy

We have determined the spectral dependence of the temporal point spread functions of human tissues experimentally between 740 and 840 nm in transmittance measurements on the adult head, forearm, and calf (*in vivo*) and the infant head (*post mortem*) by using picosecond laser pulses and a streak camera detector. Two parameters are extracted from the temporal point spread function; the differential path-length factor (DPF), calculated from the mean time, and the slope of the logarithmic intensity decay. In all tissues the DPF and the logarithmic slope show a reciprocal relationship and exhibit characteristics of the absorption spectra of hemoglobin. The DPF falls with increasing wavelength, the variation being typically 12%, while the logarithmic slope increases with wavelength. A quantitative analysis of the logarithmic slope spectrum significantly underestimated expected tissue chromophore concentrations. The absolute magnitudes of the DPF showed considerable intersubject variation, but the variation with wavelength was consistent and thus may be used in the correction of tissue attenuation spectra.

*Key words:* Near infrared, time resolved, spectroscopy, tissue, differential path length.

## 1. Introduction

Near-infrared (NIR) spectroscopy is being used increasingly for the determination of tissue oxygenation and metabolism. In particular, quantitative monitoring of the cerebral oxygenation of newborn infants has been made possible both by the technical development of dedicated spectrophotometers and by new methods to determine the effective optical path length that light takes through highly scattering tissues.

The technical development of instruments for NIR spectroscopy<sup>1-3</sup> was triggered by an experimental observation of Jöbsis,<sup>4</sup> who showed that it was possible to relate changes observed in the attenuation of NIR light (700–1000 nm) to variations in tissue oxygenation. In this wavelength region tissue atten-

uation is sufficiently low to enable optical measurements to be made across several centimeters of tissue, while the oxygen-dependent spectral changes of the chromophores hemoglobin and cytochrome *aa<sub>3</sub>* are still observable. Instruments are now commercially available that can measure these spectral changes at the bedside (NIRO 1000/NIRO 500, Hamamatsu Photonics K.K., Japan; INVOS 3100, Somanetics Corporation, USA), the only attachment to the patient being small optical fibers (optodes). The multiple scattering of light by tissues gives rise to an unknown degree of light loss, and it is, therefore, not possible to quantify the absolute concentration of these chromophores from the measured tissue attenuation spectrum. However, it is possible to apply a modified Beer–Lambert law to quantify changes in chromophore concentration from the measured changes in attenuation.<sup>5</sup> This modified law uses the differential path length (DP or  $\beta$ ), which is defined as the local gradient of the attenuation versus the absorption coefficient relationship in the tissue.<sup>6,7</sup> A number of experimental techniques have been suggested to determine this differential path length. For example, measurement of the tissue absorption arising from the known concentration of water,<sup>8,9</sup> monitoring of the phase shift of a frequency modulated light source,<sup>10,11</sup> or measurement of the direct time of flight of picosecond light pulses traveling

---

M. Essenpreis, C. E. Elwell, M. Cope, and D. T. Delpy are with the Department of Medical Physics and Bioengineering, University College London, Shropshire House, 11-20 Capper Street, London WC1E 6JA, UK; P. van der Zee is with the Division of Physical Sciences, University of Hertfordshire, College Lane, Hatfield, Herts. AL10 9AB, UK. S. R. Arridge is with the Department of Computer Science, University College London, Gower Street, London WC1, UK.

Received 15 November 1991.

0003-6935/93/040418-08\$05.00/0.

© 1993 Optical Society of America.

through tissue<sup>5</sup> have all been shown to provide this information. In this paper we discuss measurements made by the latter technique and some of the data that can be obtained from the temporal point spread function (TPSF), which is defined as the temporal response of an object to an input impulse function in light intensity.

In previous studies the mean distance traveled across the tissue by a picosecond light pulse has been shown to be an excellent approximation to the differential path length. This distance, when divided by the geometric distance between the optodes, gives a dimensionless multiplying factor, the differential path-length factor (DPF or  $B$ ), which is approximately constant for a given tissue and virtually independent of optode spacing once this exceeds 25 mm.<sup>12,13</sup> Experimentally measured values for the DPF at one wavelength have been reported previously for the adult forearm, calf, and head and for the head of the preterm infant.<sup>13,14</sup>

In this paper the question of the wavelength dependence of the TPSF is addressed, since it is known both from theoretical considerations and from experiment that this is affected by the absorption and the scattering coefficients of the tissue.<sup>5,15,16</sup> Two parameters are extracted from the TPSF, the mean time delay between light entering and leaving the tissue at given points ( $\langle t \rangle$ ) and the logarithmic slope of the intensity decay  $K_{ls}$ . A wavelength-dependent TPSF has implications for the distortion of the absorption spectra of hemoglobin and cytochrome  $aa_3$  when observed *in vivo* and hence on the algorithm used to calculate the concentrations of these chromophores from the measured changes in the tissue attenuation spectrum. A theoretical analysis of this problem has been reported,<sup>6</sup> and when measured values for the optical properties of the adult rat brain were used, the wavelength dependence of the differential optical path length was predicted.<sup>7</sup>

In this study we report experimental measurements of the TPSF between 740 and 840 nm *in vivo* on the adult head, calf, and forearm and postmortem on the head of newborn infants.

## 2. Experimental Method

A picosecond laser system together with a synchroscan streak camera (Hamamatsu Photonics, C1587) was used to record the temporal response to a short light pulse entering the tissue (Fig. 1). The laser system consisted of a 12-W Ar-ion laser (Spectra Physics, 2040) pumping a Ti:sapphire laser (Spectra Physics, Tsunami), which was tunable between 740 and 840 nm. The auto-mode-locking behavior of the Ti:sapphire crystal in this laser was supported by an electro-optical feedback mechanism resulting in a stable mode locking at 82 MHz and a full width at half-maximum of a single pulse of  $\sim 2$  ps. The light was coupled into a single low-dispersion fiber (Corning SDF, 125  $\mu\text{m}$  in diameter, 0.6 m in length) to allow easy application of light to the tissue. Part of

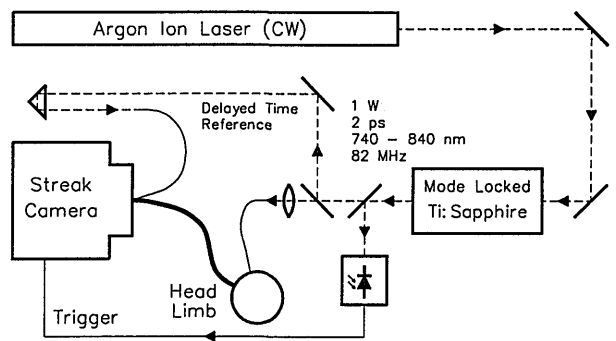


Fig. 1. Experimental system for the measurement of the TPSF in tissue.

the laser output was sampled both as a time reference and as a trigger for the streak camera. Light emerging from the tissue was collected with a fiber bundle having a circular cross section (1.9 mm in diameter) at the tissue end and a linear cross section at the distal end, which matched the streak camera input slit. The fiber bundle was assembled from 100 single low-dispersion fibers (Corning SDF), each 1000 mm ( $\pm 1$  mm) long to minimize transit time differences. The overall temporal resolution of the system was 10 ps. The effects of color delays were eliminated by the simultaneous recording of a temporal reference and the sample on the same streak image.

### A. Temporal Point Spread Function

A typical tissue response to the picosecond light pulse is shown in Fig. 2. The data were collected at 760 nm from the head of an adult (with optode spacing of 40 mm). The TPSF was characterized by two parameters: the mean time  $\langle t \rangle$  and the gradient of the decay of the logarithmic intensity  $K_{ls}$ .

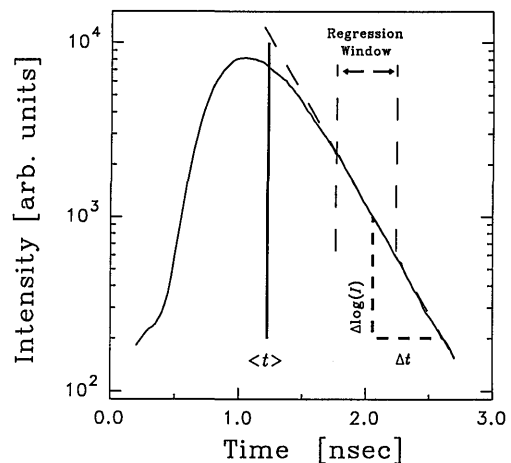


Fig. 2. Typical temporal point spread function measured on the head of an adult showing the mean time  $\langle t \rangle$  and the calculation of  $K_{ls}$ .

### B. Differential Path-Length Factor $B$

The mean transit time of the photons in the tissue is defined as

$$\langle t \rangle = \frac{\int_0^{\infty} tI(t)dt}{\int_0^{\infty} I(t)dt}, \quad (1)$$

where  $I(t)$  is the intensity of the light recorded by the streak camera as a function of time  $t$ . Since the TPSF was measured over a finite temporal window and the streak camera collected the light in discrete channels, the integral in Eq. (1) is approximated by a finite sum:

$$\langle t \rangle = \frac{\tau \sum_{k=1}^n kI(k)}{\sum_{k=1}^n I(k)}. \quad (2)$$

Here  $\tau$  is the time calibration of the streak camera ( $\tau = 4.95$  ps/channel) and  $n$  is the total number of data channels ( $n = 512$ ).

The differential path-length factor  $B$  is defined as  $\beta/d$ , where  $d$  is the physical distance between the transmitting fiber and the center of the detecting fiber bundle and  $\beta$  is the differential path length, but in terms of time-of-flight measurements it can be approximated by

$$B = \frac{\beta}{d} \approx \frac{1}{d} \frac{c}{n_t} \langle t \rangle, \quad (3)$$

where  $c$  is the speed of light in vacuum and  $n_t$  is the refractive index of the tissue. (For all the measurements described in this paper a value for  $n_t$  of 1.40 was assumed.<sup>17</sup>)

### C. Logarithm Slope $K_{Is}$

The second parameter used to characterize the TPSF is the gradient in a logarithmic plot of the intensity decay with time ( $\text{cm}^{-1}$ ):

$$K_{Is} = - \frac{\Delta \log[I(t)]}{\Delta l} = - \frac{n_t}{c} \frac{\Delta \log[I(t)]}{\Delta t}, \quad (4)$$

where  $\Delta l = \Delta t \times c/n_t$ . As can be seen in Fig. 2, after rising to an initial peak, the TPSF intensity falls linearly with time in a logarithmic plot. The slope of this decay was calculated from a linear regression performed in a window defined by percentages of the intensity maximum. This was 10% for the start of the regression and 2% for the end. Several publications have suggested that this exponential decay can be understood as a time-resolved Beer-Lambert law, and thus  $K_{Is}$  equals  $\mu_a$ , the absorption coefficient of the tissue.<sup>18,19</sup> However, to equate the two is clearly

an oversimplification since  $K_{Is}$  also depends on  $\mu_s$ , the scattering coefficient of the tissue, and on the measurement geometry.<sup>20-23</sup>

### 3. Subjects and Experimental Procedure

In line with previous studies<sup>13</sup> the TPSF has been measured on the head, forearm, and calf of each of a group of adult volunteers (male and female). The subjects were between 18 and 55 (median 26) years of age with no known muscular or circulatory disorders. Details for each group are given in Section 4. Typically a wavelength scan consisted of 13 separate measurements made over a range of 740–840 nm and took  $\sim 30$  min. For measurements on the leg or arm the subjects were seated comfortably and the limb was placed in a U-shaped rest into which holes were drilled that enabled both the transmitting and the receiving fibers to be placed in contact with the skin from below. The fibers were positioned over the muscles either on the medial aspect of the forearm away from any palpable bone or on the rear surface of the calf muscle at the broadest part of the leg. The optode spacing was  $\sim 40$  mm for all the studies. Care was taken that the blood supply to the tissues was not obstructed while the limb lay in the apparatus by supporting the wrist or heel on an adjustable rest. Background light was reduced by wrapping the limb with a black cloth.

A slightly modified procedure was applied for the measurements made on the head. First, an elasticated strap was wrapped around the head, attached to which, at 1-cm intervals, were small black plastic blocks. The holes in these blocks permitted the fibers to be placed in contact with the skin surface. The strap was positioned on the right upper forehead just below the hairline. The receiving fiber was then positioned over the temple with the transmitting fiber on the forehead  $\sim 40$  mm away. To avoid movements during measurements, the subject sat in a reclining position in a chair that also supported the head. After the TPSF measurements were completed, the fibers were removed and their position on the skin was marked with a pen placed through the holes in the plastic blocks. After removing the strap, we measured the distance between the marks on the skin by using callipers. The accuracy of this measurement of the interoptode spacing was estimated to be  $\pm 2$  mm.

The heads of two infants were studied *post mortem*. Infant 1 was an unexpected stillbirth at 41 weeks of gestation. There was no ultrasound evidence of cerebral hemorrhage. The measurements were carried out 62 h after delivery. Infant 2 was born at 27 weeks of gestation and died at 15 days. Ultrasound examination showed bilateral hemorrhagic parenchymal infarction. This infant was studied 34 h after death. Both infants were kept at 4°C between death and examination.

## 4. Results

### A. Adult Head

Measurements were made on seven subjects [six male, one female, 23–55 (median 28) years old]. Figure 3 shows the TPSF at several wavelengths as measured on one subject. The change in both the position and shape of the TPSF with wavelength can be seen clearly. The results from the heads of all subjects are shown in Fig. 4. In Fig. 4(a) the calculated value of the DPF as a function of wavelength is shown. For all subjects there is a marked local minimum at 760 nm, which coincides with an NIR absorption peak of deoxygenated hemoglobin.<sup>8</sup> In contrast the corresponding values of  $K_{ls}$  exhibit a local maximum at 760 nm [Fig. 4(b)]. Both the DPF and  $K_{ls}$  display an extremely similar wavelength dependence in all subjects, although there is a considerable spread in the absolute magnitude. Note that more frequent wavelength sampling was applied around the 760-nm peak. Figure 5 summarizes the results from the adult head obtained by averaging the data from all the subjects. The original data for each subject were linearly interpolated to 5-nm intervals; then the values for the DPF's were normalized to their values at 800 nm. The averages and standard deviations of the normalized data were then calculated. The average value of all DPF's at 800 nm ( $\langle B_{800} \rangle$ ) was  $6.32 \pm 0.46$ .

The same procedure was applied to the  $K_{ls}$  data, but we rescaled the average values by multiplying with the average value at 800 nm. The reference wavelength of 800 nm was chosen for practical reasons since it falls within the overlap region of the mirror sets of the Tsunami laser. (Mirrors are now available for wavelength ranges of 720–840 and 780–900 nm.) Future measurements in the 780–900-nm region can thus be matched to the data described here. The averaged data show more clearly the local maximum in  $K_{ls}$  and the minimum in DPF at 760 nm.

### B. Adult Forearm

Measurements were made on six subjects [four male, two female, 24–55 (median 26) years old]. The aver-

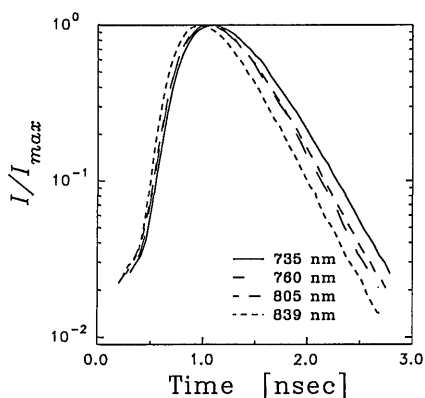


Fig. 3. Temporal point spread functions measured at several wavelengths on the head of one subject (optode spacing 40 mm).

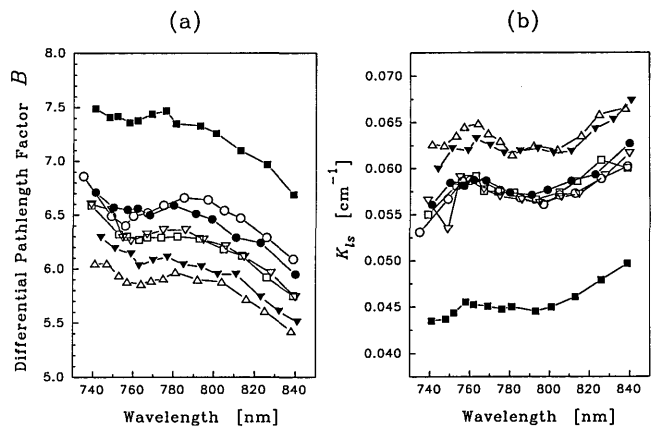


Fig. 4. Changes with wavelength (a) in the differential pathlength factor and (b) in  $K_{ls}$  measured on the heads of all subjects.

age results for all subjects are shown in Fig. 6. The same wavelength-dependent behavior of DPF and  $K_{ls}$  can be seen. But the overall magnitude of the DPF is significantly lower compared with the head ( $\langle B_{800} \rangle = 4.48 \pm 0.41$ ). Note that the values for  $K_{ls}$  are the highest observed in any of the adult tissues studied.

### C. Adult Calf

In a previous study a difference in the value of the DPF between male and female subjects had been observed.<sup>13</sup> Measurements were, therefore, made on six male [25–36 (median 26) years old] and six female [18–32 (median 23) years old] subjects. The data for the DPF and  $K_{ls}$  for male and female calves are plotted in Figs. 7(a) and 7(b). Again there is a considerable variation in both with wavelength. However, in contrast with the earlier study there was no significant difference in the results between the male and female calf, the value for  $\langle B_{800} \rangle$  being  $5.84 \pm 0.65$  in male and  $5.63 \pm 0.62$  in female subjects.

### D. Infant Head

Figure 8 shows the values of DPF and  $K_{ls}$  for the heads of the two infants studied *post mortem*. As

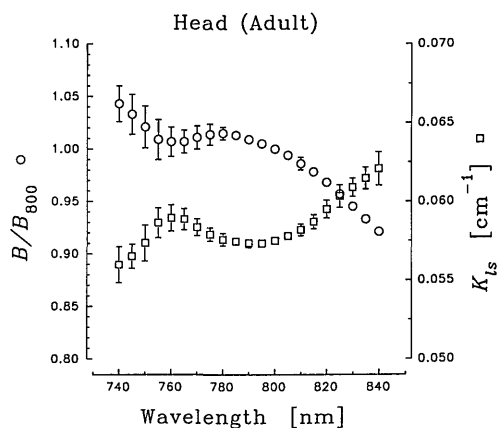


Fig. 5. Changes with wavelength of the normalized DPF and  $K_{ls}$  in the adult head. Data are the average for all subjects  $\pm 1$  standard deviation.

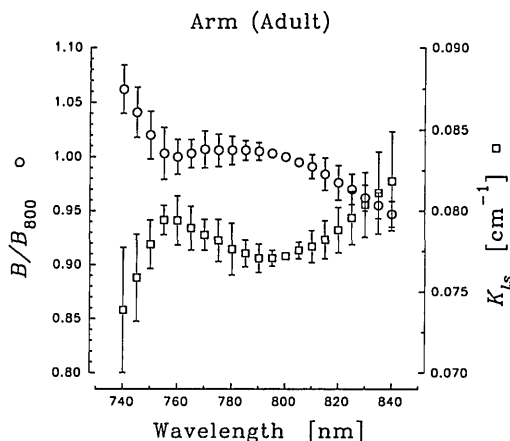


Fig. 6. Changes with wavelength of the normalized DPF and  $K_{ls}$  in the adult forearm. Data are the average for all subjects with  $\pm 1$  standard deviation.

expected both the local minimum in the DPF and the local maximum in  $K_{ls}$  at 760 nm are larger than in the data from the normoxic adult brain. The magnitude of the DPF is considerably less in the infant head than in the adult, a result that has been observed in previous studies.<sup>13,14</sup>

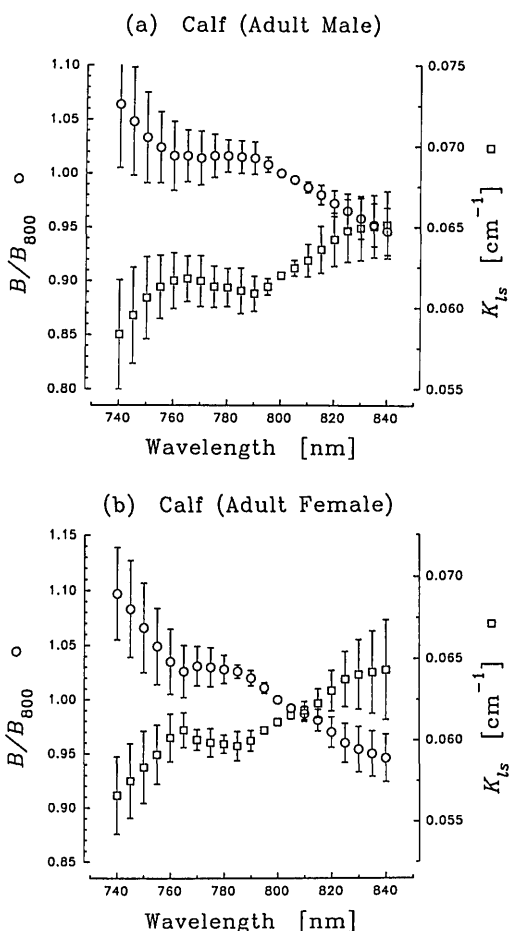


Fig. 7. Changes with wavelength of the normalized DPF and  $K_{ls}$  in the male and (b) in the female adult calf. Data are the average for all subjects  $\pm 1$  standard deviation.

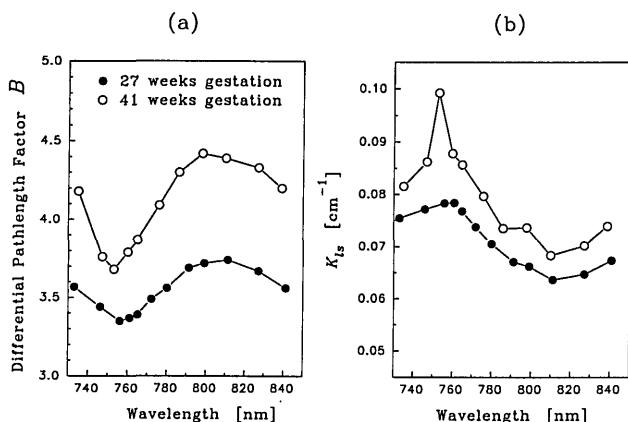


Fig. 8. Change with wavelength (a) in the DPF and (b) in  $K_{ls}$  measured on the head of two infants *post mortem*.

## 5. Discussion

The wavelength dependence of the DPF and  $K_{ls}$  in the normoxic adult head, calf, and forearm all show similar characteristics. When normalized to its value at 800 nm, the DPF shows a small dip of 3–5% at 760 nm, which is caused by the presence of deoxyhemoglobin. The effect of this absorption peak is also seen as a corresponding increase in  $K_{ls}$  at 760 nm. These effects are more pronounced in the data from the postmortem infants, where presumably all the blood in the head is deoxygenated. It is not surprising to find that the wavelength dependence of the DPF and  $K_{ls}$  are approximately mirror images of each other as an increase in  $\mu_a$  has been shown both theoretically and experimentally to reduce the DPF.<sup>16</sup>

The other wavelength-dependent feature of the DPF, observed on all tissues, is a gradual decrease with increasing wavelength. The variation is  $\pm 6\%$  over a range of 100 nm. The reasons for this are twofold. First, in normoxic tissues the percentage of oxygenated hemoglobin and myoglobin will exceed that of the deoxygenated compounds. Beyond 800 nm the absorption coefficient of the oxygenated chromophores increases with wavelength.<sup>8</sup> This, together with the increase in water absorption with wavelength, will lead to the DPF falling with increasing wavelength. Second, experimental measurements of the scattering properties of tissues show a gradual decrease in  $\mu_s$  with wavelength.<sup>24,25</sup> Diffusion theory predicts that this decrease will lead to a reduction in the DPF.<sup>7</sup>

The wavelength dependence of the DPF in the rat brain was predicted previously<sup>7</sup> when diffusion theory was applied to values of  $\mu_a$  and  $\mu_s$  experimentally measured on thin slices of rat brain tissue. The data presented here are the first experimentally determined spectra of the wavelength dependence of the DPF. In its normalized form the experimental data for the adult brain match that predicted for the adult rat brain. The small differences between the experimentally measured and the theoretically predicted data could arise for a number of reasons. First, the data for the optical coefficients of the tissue are

measured *post mortem* and on a different species. Second, diffusion theory calculations were performed on the basis of an infinite medium, and to apply the results to the actual geometry of the head will introduce errors because of boundary effects and the presence of other tissues (e.g., the skull).

The error bars in Figs. 5–7 represent wavelength-dependent variations between subjects. This wavelength dependence could arise from changes in tissue hemodynamics or small movements of the subject occurring during the 30-min measurement period. These effects were minimized by keeping the subjects still and relaxed. A more likely reason would be differences in the normoxic concentrations of oxyhemoglobin ( $\text{HbO}_2$ ) and deoxyhemoglobin (Hb) resulting from different tissue blood volume and oxygenation.

The absolute values of the DPF in all the studies showed a considerable subject-to-subject variation. Some of this variation, especially in the data from the head, may arise from errors in the measurement with the callipers of the interoptode spacing. However, the measurements on the forearm and calf were made with a positioning assembly that ensured a much more consistent fiber placement. (Repeated studies on a subject have shown little variation in DPF over 1 h.<sup>13</sup>) The differences observed here, therefore, reflect true intersubject variation. These may arise from small variations in the optical properties of specific types of tissue<sup>24,26,27</sup> but most probably reflect gross variations in anatomy and tissue composition<sup>28</sup> (e.g., variations in skull thickness or the fat/muscle ratio). No correlation has been observed between the object diameter and the measured DPF.

The value of  $K_{ls}$  was previously interpreted as the tissue absorption coefficient.<sup>19</sup> Diffusion theory predicts that the value of  $K_{ls}$  should be proportional to absorption coefficient  $\mu_a$ , but the two are equal only in extremely limited circumstances.<sup>21–23</sup>  $K_{ls}$  asymptotically approaches  $\mu_a$  in the case only of an infinite medium at infinite time. We can see the problems of equating  $K_{ls}$  and  $\mu_a$  by analyzing the contribution of tissue chromophore absorption to the measured  $K_{ls}$  spectrum. If assumptions are made both that  $K_{ls} = \mu_a$  and that  $\mu_a$  at these wavelengths is composed solely of Hb,  $\text{HbO}_2$ , cytochrome  $aa_3$  (oxidized), and water, then the  $K_{ls}$  spectrum should consist of a linear sum of the absorption spectra of these compounds.<sup>8,9,29</sup> We tested this hypothesis on the  $K_{ls}$  data from the adult brain using a constrained nonlinear regression analysis<sup>30</sup> to determine their relative contributions (dashed curve, Fig. 9). The constraint was that all concentrations be positive. The regression yielded concentrations of 9  $\mu\text{M}$  for Hb and 0.0  $\mu\text{M}$  for  $\text{HbO}_2$  (molecular weight 64,500 u) and 14  $\mu\text{M}$  for cytochrome  $aa_3$  (the functional unit). The figure for the water concentration was 53% by volume. These values are obviously incorrect, and the spectral fit is poor ( $R^2 = 0.83$ ). A typical value for the total hemoglobin concentration (Hb +  $\text{HbO}_2$ ) in the adult brain is 84  $\mu\text{M}$ .<sup>31</sup> The expected cytochrome  $aa_3$  concentra-

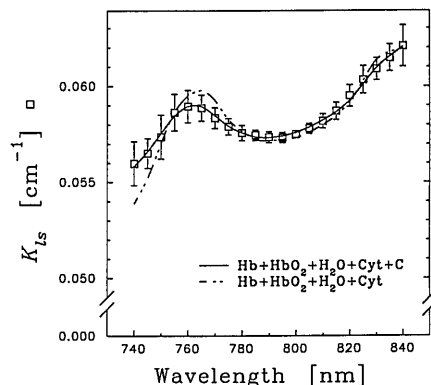


Fig. 9.  $K_{ls}$  spectrum taken from Fig. 5 together with the results of two constrained nonlinear regressions (see text for details).

tion, estimated from adult rat brain measurement, is 5  $\mu\text{M}$ ,<sup>32</sup> and the water content is typically 80% by volume.<sup>33</sup> The spectral fit can be improved considerably (solid curve, Fig. 9) if a further term is added to the regression. In the illustrated case a simple constant has been added improving  $R^2$  to 0.995. The regression then yielded the following concentrations: 5  $\mu\text{M}$  (Hb), 16  $\mu\text{M}$  ( $\text{HbO}_2$ ), 0.0  $\mu\text{M}$  (cytochrome  $aa_3$ ), 23% (water), and a constant term of 0.038  $\text{cm}^{-1}$ . All values underestimate severely the expected concentrations by a factor of 3–4 times. However, despite a total hemoglobin concentration of only 21  $\mu\text{M}$ , it is interesting to note that the calculated brain tissue hemoglobin saturation [ $\text{HbO}_2/(\text{Hb} + \text{HbO}_2)$ ] was 76%, a value similar to that obtained by other methods.<sup>11,34</sup>

The fact that a background constant is required to obtain an adequate fit to the experimental  $K_{ls}$  data is not surprising. In this case its exact origins are unknown but are likely to arise from light scattering and the finite object size<sup>23</sup> and from absorption by other chromophores. The rather low values of all chromophore concentrations are more surprising and cannot be explained easily. It is difficult to find errors in the experimental technique, absolute values of  $K_{ls}$  agree with those reported by other researchers,<sup>18,19</sup> and the wavelength spectrum was sampled adequately to resolve the 760-nm peak of deoxyhemoglobin. From the expected tissue chromophore concentrations the minimum tissue absorption coefficient was calculated to be 0.095  $\text{cm}^{-1}$  (at 800 nm).  $K_{ls}$  should, therefore, be at least as large as this value. Other authors have also found problems in attempting to calculate  $\mu_a$  from the TPSF.<sup>23</sup> In these latter studies TPSF's were measured in phantoms in highly controlled conditions of  $\mu_a$ ,  $\mu_s$  and in a semi-infinite geometry. However, the value of  $\mu_a$  estimated by using the diffusion equation to fit the experimental TPSF's was 10% below the correct value. Both pieces of evidence indicate that  $\mu_a$  cannot be equated simply to  $K_{ls}$  as originally thought and that more work is required to establish how the TPSF can be used to determine the absolute concentrations of Hb and  $\text{HbO}_2$  in tissue.

## 6. Conclusions

The spectral dependence of the logarithmic slope data agreed with theoretical predictions,  $K_{ls}$  increasing with longer wavelength and a local maximum at 760 nm, coinciding with the absorption peak of deoxyhemoglobin. However, attempts to quantitate chromophore concentrations from the  $K_{ls}$  data resulted in a severe underestimation. Further theoretical and experimental work is required to investigate this anomaly.

The significance of the DPF was established previously, and it has been used clinically to derive cerebral blood flow<sup>35</sup> and cerebral blood volume<sup>36</sup> from NIR spectroscopy data. The intersubject variation in DPF observed in this and other studies places a limit on the accuracy of these quantitative measurements (typically  $\pm 10\%$ ). This source of error can be avoided if the differential path length is measured on each patient.

One major advantage of NIR spectroscopy is that in theory it can measure the redox state of cytochrome  $aa_3$ . Problems in the determination of cytochrome concentration from the NIR data have been described previously,<sup>7</sup> and an improved accuracy of determination has been demonstrated when a differential pathlength that is both wavelength and absorption coefficient dependent is used. The wavelength dependence of the DPF has now been measured and in principle could be used to correct for the spectral distortions that arise when we measure in tissue. The standard deviations of the normalized DPF spectra are small, showing a maximum value of 5.5% for muscle and 2.0% for brain. This suggests that only one normalized DPF spectrum per organ or limb may be needed to correct for wavelength-dependent effects. The advantage of this approach to the analysis of NIR data is that spectral distortion can be traced to its physical basis, i.e., optical path-length variations. For practical use in most NIR spectrometers the DPF spectrum requires extension to 910 nm. This should be possible in the near future with the availability of other optics for the Tsunami laser.

The work described here was supported by grants from the Wellcome Trust, the Science and Engineering Research Council, the Medical Research Council, the Wolfson Foundation, and Hamamatsu Photonics K.K. We thank Spectra Physics, U.K. for the loan of the Tsunami laser system.

## References and Notes

1. M. Cope and D. T. Delpy, "A system for long term measurement of cerebral blood and tissue oxygenation in newborn infants by near infrared transillumination," *Med. Biol. Eng. Comput.* **26**, 289–294 (1988).
2. P. A. Rea, J. Crowe, Y. Wickramasinghe, and P. Rolfe, "Non invasive optical methods for the study of cerebral metabolism in the human newborn: a technique for the future?" *J. Med. Eng Technol.* **9**, 160–166 (1985).
3. I. Giannini, M. Ferrari, A. Carpi, and P. Fasella, "Rat brain monitoring by near infrared spectroscopy: an assessment of possible clinical significance," *Physiol. Chem. Phys.* **14**, 295–305 (1982).
4. F. F. Jöbsis, "Non invasive, infrared monitoring of cerebral and myocardial oxygen sufficiency and circulatory parameters," *Science* **198**, 1264–1267 (1977).
5. D. T. Delpy, M. Cope, P. van der Zee, S. R. Arridge, S. Wray, and J. S. Wyatt, "Estimation of optical pathlength through tissue from direct time of flight measurement," *Phys. Med. Biol.* **33**, 1433–1442 (1988).
6. M. Cope, "The development of a near infrared spectroscopy system and its application for non invasive monitoring of cerebral blood and tissue oxygenation in the newborn infant, Ph.D. dissertation (University of London, London, 1991).
7. M. Cope, P. van der Zee, M. Essenpreis, S. R. Arridge, and D. T. Delpy, "Data analysis methods for near infrared spectroscopy of tissue: problems in determining the relative cytochrome  $aa_3$  concentration," in *Time-Resolved Spectroscopy and Imaging of Tissues*, B. Chance, ed., *Proc. Soc. Photo-Opt. Instrum. Eng.* **1431**, 251–262 (1991).
8. S. Wray, M. Cope, D. T. Delpy, J. S. Wyatt, and E. O. R. Reynolds, "Characterization of the near infrared absorption spectra of cytochrome  $aa_3$  and hemoglobin for the noninvasive monitoring of cerebral oxygenation," *Biochim. Biophys. Acta* **933**, 184–192 (1988).
9. M. Cope, D. T. Delpy, S. Wray, J. S. Wyatt, and E. O. R. Reynolds, "A CCD spectrometer to quantitate the concentration of chromophores in living tissue utilising the absorption peak of water at 975 nm," *Adv. Exp. Med. Biol.* **248**, 33–40 (1989).
10. J. R. Lakowicz and K. Berndt, "Frequency domain measurements of photon migration in tissues," *Chem. Phys. Lett.* **166**, 246–252 (1990).
11. E. M. Sevick and B. Chance, "Photon migration in a model of the head measured using time and frequency domain techniques: potentials of spectroscopy and imaging," in *Time-Resolved Spectroscopy and Imaging of Tissues*, B. Chance, ed., *Proc. Soc. Photo-Opt. Instrum. Eng.* **1431**, 84–96 (1991).
12. P. van der Zee, S. R. Arridge, M. Cope, and D. T. Delpy, "The effect of optode positioning on optical pathlength in near infrared spectroscopy of brain," *Adv. Exp. Med. Biol.* **277**, 79–84 (1990).
13. P. van der Zee, M. Cope, S. R. Arridge, M. Essenpreis, L. A. Potter, A. D. Edwards, J. S. Wyatt, D. C. McCormick, S. C. Roth, E. O. R. Reynolds, and D. T. Delpy, "Experimentally measured optical pathlengths for the adult head, calf and forearm and the head of the newborn infant as a function of interoptode spacing," *Adv. Exp. Med. Biol.* (to be published).
14. J. S. Wyatt, M. Cope, D. T. Delpy, P. van der Zee, S. R. Arridge, A. D. Edwards, and E. O. R. Reynolds, "Measurement of optical pathlength for cerebral near infrared spectroscopy in newborn infants," *Dev. Neurosci.* **12**, 140–144 (1990).
15. M. Ferrari, R. A. De Blasi, P. Bruscaioni, M. Barilli, L. Carraresi, M. Gurioli, E. Quaglia, and G. Zaccanti, "Near infrared time-resolved spectroscopy and fast scanning spectrophotometry in ischemic human forearm," in *Time-Resolved Spectroscopy and Imaging of Tissues*, B. Chance, ed., *Proc. Soc. Photo-Opt. Instrum. Eng.* **1431**, 276–283 (1991).
16. D. T. Delpy, S. R. Arridge, M. Cope, A. D. Edwards, E. O. R. Reynolds, C. E. Richardson, S. Wray, J. S. Wyatt, and P. van der Zee, "Quantitation of pathlength in optical spectroscopy," *Adv. Exp. Med. Biol.* **248**, 41–46 (1989).
17. F. P. Bolin, L. E. Preuss, R. C. Taylor, and R. Ference, "Refractive index of some mammalian tissues using a fiber optic cladding method," *Appl. Opt.* **28**, 2297–2302 (1989).
18. B. Chance, J. S. Leigh, H. Miyake, D. S. Smith, S. Nioka, R. Greenfeld, M. Finander, K. Kaufmann, W. Levy, M. Young, P. Cohne, H. Yoshioka, and R. Boretsky, "Comparison of time resolved and unresolved measurements of deoxyhemoglobin in brain," *Proc. Natl. Acad. Sci. USA* **85**, 4971–4975 (1988).
19. B. Chance, S. Nioka, J. Kent, K. McCully, M. Fountain, R.

- Greenfeld, and G. Holtom, "Time resolved spectroscopy of haemoglobin and myoglobin in resting and ischaemic muscle," *Anal. Biochem.* **174**, 698–707 (1988).
20. R. Nossal, and R. F. Bonner, "Differential time-resolved detection of absorbance changes in composite structures," in *Time-Resolved Spectroscopy and Imaging of Tissues*, B. Chance, ed., Proc. Soc. Photo-Opt. Instrum. Eng. **1431**, 21–28 (1991).
  21. M. S. Patterson, J. D. Moulton, B. C. Wilson, and B. Chance, "Applications of time resolved light scattering measurements to photodynamic therapy dosimetry," in *Photodynamic Therapy: Mechanisms II*, T. J. Dougherty, ed., Proc. Soc. Photo-Opt. Instrum. Eng. **1203**, 62–75 (1990).
  22. S. L. Jacques and S. T. Flock, "Effect of surface boundary on time resolved reflectance: measurement with a prototype endoscopic catheter," in *Time-Resolved Spectroscopy and Imaging of Tissues*, B. Chance, ed., Proc. Soc. Photo-Opt. Instrum. Eng. **1431**, 12–20 (1991).
  23. S. J. Madsen, M. S. Patterson, B. C. Wilson, Y. D. Park, J. D. Moulton, S. L. Jacques, and Y. Hefetz, "Time resolved diffuse reflectance and transmittance studies in tissue simulating phantoms: a comparison between theory and experiment," in *Time-Resolved Spectroscopy and Imaging of Tissues*, B. Chance, ed., Proc. Soc. Photo-Opt. Instrum. Eng. **1431**, 42–51 (1991).
  24. P. van der Zee, M. Essenpreis, D. T. Delpy, and M. Cope, "Accurate determination of the optical properties of biological tissues using a Monte Carlo inversion technique," presented at the International Commission for Optics Meeting on Atmospheric, Volume and Surface Scattering and Propagation, Florence, Italy, 27–30 August 1991.
  25. H. J. C. M. Sterenborg, M. J. C. van Gemert, W. Kamphorst, J. G. Wolbers, and W. Hogervorst, "The spectral dependence of the optical properties of human brain," *Lasers Med. Sci.* **4**, 221–227 (1989).
  26. J. L. Karagiannes, Z. Zhang, B. Grossweiner, and L. I. Grossweiner, "Applications of the 1-D diffusion approximation to the optics of tissues and tissue phantoms," *Appl. Opt.* **28**, 2311–2317 (1989).
  27. R. Marchesini, A. Bertoni, S. Andreola, E. Melloni, and A. E. Sichirollo, "Extinction and absorption coefficients and scattering phase functions of human tissues *in vitro*," *Appl. Opt.* **28**, 2318–2324 (1989).
  28. R. J. Maughan, J. S. Watson, and J. Weir, "The relative proportions of fat, muscle and bone in the normal human forearm as determined by computer assisted tomography," *Clin. Sci.* **66**, 683–689 (1984).
  29. M. Brunori, E. Antonini, and M. T. Wilson, "Cytochrome c oxidase: an overview of recent work," in *Metal Ions in Biological Systems XIII*, H. Siegel, ed. (Marcel Dekker, New York, 1981).
  30. SPSS, Inc., 444 North Michigan Avenue, Chicago, Ill. 60611 (1990).
  31. F. Sakai, K. Nakazawa, Y. Tazaki, K. Ishii, H. Hidetada, H. Igarashi, and T. Kanda, "Regional cerebral blood volume and hematocrit measured in normal human volunteers by single-proton emission computed tomography," *J. Cereb. Blood Flow Metab.* **5**, 207–213 (1985).
  32. G. C. Brown, M. Crompton, and S. Wray, "Cytochrome oxidase content of rat brain during development," *Biochim. Biophys. Acta.* **1057**, 273–275 (1991).
  33. G. Brant, "Studies on lipids in the nervous system with special reference to quantitative chemical determination and topical distribution," *Acta. Physiol. Scand.* **18** Suppl. 63, 1–189. (1949).
  34. P. W. McCormick, M. Stewart, M. G. Goetting, M. Dujovny, G. Lewis, and J. I. Ausman, "Noninvasive cerebral optical spectroscopy for monitoring cerebral oxygen delivery and hemodynamics," *Crit. Care Med.* **19**, 89–97 (1991).
  35. A. D. Edwards, J. S. Wyatt C. E. Richardson, D. T. Delpy, M. Cope, and E. O. R. Reynolds, "Cotside measurements of cerebral blood flow in ill newborn infants by near infrared spectroscopy," *Lancet* **ii**, 770–771 (1988).
  36. J. S. Wyatt, M. Cope, D. T. Delpy, C. E. Richardson, A. D. Edwards, S. C. Wray, and E. O. R. Reynolds, "Quantitation of cerebral blood volume in newborn infants by near infrared spectroscopy," *J. Appl. Physiol.* **68**(3), 1086–1091 (1990).